

PF-FLO REFERENCE TEST  
AT THE  
MARTIN-LUTHER UNIVERSITY HALLE-WITTENBERG

Martin-Luther-Universität Halle-Wittenberg  
Fachbereich Ingenieurwissenschaften  
Lehrstuhl für Mechanische Verfahrenstechnik  
06099 Halle (Saale)  
Germany

AMC Power – PROMECON  
1050 Hopper Avenue  
Santa Rosa, California 95403  
U.S.A.

# PF-FLO REFERENCE TEST AT THE MARTIN-LUTHER UNIVERSITY HALLE-WITTENBERG

CONTENTS	Page
<a href="#">1. Introduction</a> .....	1
<a href="#">2. Description of the Test Facilities</a> .....	3
<a href="#">2.1 The Testing Plant</a> .....	3
<a href="#">2.2 The Pf-FLO Mass Flow Measurement</a> .....	4
<a href="#">2.2.1 Density measurement</a> .....	4
<a href="#">2.2.2 Velocity measurement</a> .....	5
<a href="#">2.2.3 Calculation of the Mass Flow</a> .....	6
<a href="#">2.3 Pf-FLO Test Configuration</a> .....	6
<a href="#">2.4 The Test Medium</a> .....	8
<a href="#">2.5 Feeder Calibration</a> .....	9
<a href="#">3. Testing Procedure</a> .....	11
<a href="#">4. Results</a> .....	14
<a href="#">4.1 Pf-FLO Measurement Accuracy</a> .....	14
<a href="#">4.1.1 Absolute Deviation</a> .....	15
<a href="#">4.1.2 Repeatability</a> .....	16
<a href="#">4.2 Influence of the Particle Size</a> .....	17
<a href="#">4.2.1 Velocity Measurement</a> .....	17
<a href="#">4.2.2 Density Measurement</a> .....	19
<a href="#">4.2.3 Mass flow measurement</a> .....	20
<a href="#">5. Abstract</a> .....	23

<b>Figures</b>	<b>Page</b>
<a href="#">Fig. 2.1: Schematic drawing of the test plant</a> .....	3
<a href="#">Fig. 3.1: Range of pf-concentrations based on feeder mass flow and transport air flow</a> .....	11
<a href="#">Fig. 3.2: Density measurement</a> .....	12
<a href="#">Fig. 3.3: Velocity measurement</a> .....	12
<a href="#">Fig. 3.4: Resulting mass flow and feeder signal</a> .....	12
<a href="#">Fig. 3.5: Mass flow of feeder versus Pf-FLO</a> .....	12
<a href="#">Fig. 4.1: Evaluation of all test runs with 66 / 225 <math>\mu\text{m}</math> particles</a> .....	14
<a href="#">Fig. 4.2: Repeatability of channel 0 for 66 - 225 <math>\mu\text{m}</math> particles</a> .....	15
<a href="#">Fig. 4.3 Averaged particle velocities at channel 0</a> .....	17
<a href="#">Fig. 4.4: Acceleration along the test duct of the 225 <math>\mu\text{m}</math> particles</a> .....	18
<a href="#">Fig. 4.5: Influence of the mass flow on the velocity of the particle mix in Test IV-VI</a> ..	18
<a href="#">Fig. 4.6: Density measurement with 66 <math>\mu\text{m}</math> particles Test V</a> .....	19
<a href="#">Fig. 4.7: Density measurement with 225 <math>\mu\text{m}</math> particles Test I</a> .....	19
<a href="#">Fig. 4.8: Influence of the particle size on the Pf-FLO measurement</a> .....	20
<a href="#">Fig. 4.9: Estimated deviation by modeled particle size distribution</a> .....	22

<b>Tables</b>	<b>Page</b>
<a href="#">Table 2.1: Bulk density and frequency shift for fixed-bed powder of pulverized black coal and glass particles</a> .....	8
<a href="#">Table 3.1: Test run number for each particle size</a> .....	12
<a href="#">Table 4.1: Standard deviation and mean error for individual particle fractions</a> .....	15
<a href="#">Table 4.2: Standard deviation of the individual channels with 66 <math>\mu\text{m}</math> particles</a> .....	16
<a href="#">Table 4.3: Standard deviation of the individual channels with 225 <math>\mu\text{m}</math> particles</a> .....	16
<a href="#">Table 4.4: Standard deviation of the individual channels with 66-225 <math>\mu\text{m}</math> particle mix</a> .	16
<a href="#">Table 4.5: Ratio of arbitrary units to mass and the resulting mass frequency factor <math>k_{fd}</math> for each particle fraction</a> .....	21

# 1. Introduction

Measurement of particle concentration or mass flow rate in pipeline systems (i.e. pneumatic conveying) is essential for numerous technical applications, such as conveying of pulverized coal in power plants or conveying systems in cement factories. Of major importance is the detection of the particulate flow in the entire cross-section of a pipe. In the past this has generally only been achieved in pipe elements where the particulate concentration is homogeneously distributed over the entire cross-section. For such a measurement different techniques are available, namely extractive methods utilizing probes and non-extractive methods employing electromagnetic waves or particle charging. From the first inspection an isokinetic sampling probe seems to be the simplest approach, however, in order to measure the particulate flux in the entire pipe section it is necessary to systematically position the extraction probe at defined locations across the entire pipe cross-section. Due to probe erosion damage, extractive sampling is only suitable for periodic measurement. For continuous measurement, non-extractive methods are more favorable, where the sensing instrumentation is mounted in-situ. One approach is the detection of the electrostatic charge of moving particles. Unfortunately, the resulting signal is not only affected by particle concentration, but also by gas temperature and particle velocity. The method used for the investigation documented in this report is based on utilizing microwaves emitted and detected by screw-in sensors. The generated microwave field covers the entire pipe cross-section and hence allows the determination of the averaged particle concentration over that cross-section. The principle of the method will be outlined below.

The microwave based experiments were conducted on an air-particle flow loop established at the Lehrstuhl für Mechanische Verfahrenstechnik of the Martin-Luther University Halle-Wittenberg. In order to consider different conveying conditions, probes were installed at multiple locations of the conveying pipe, namely in an upward flow with almost homogeneous dust distribution, behind a vertical-horizontal bend where roping is likely to occur, and in an almost fully developed state of a horizontal pipe. The particle introduction was achieved using a calibrated screw feeder, which also allowed the comparison of the particulate mass flow with the result from the microwave instrument. Since the handling of pulverized coal could not be safely performed at the test facility, spherical glass beads of two different mean diameters were used as coal substitutes. It is acknowledged that the different material density and particle shape of the glass particles results in a slightly different conveying behavior, primarily in the form of lower particle velocities, but otherwise the general flow behavior of coal and glass particle is extremely similar.

This report presents a description of the test facility and the measurement principle. The measurements are presented in comparison with the calibrated screw feeder, and a detailed discussion of the accuracy achieved with the microwave instrument is provided.

## 2. Description of the Test Facilities

The reference test was carried out at the Merseburg test plant. The test facility is designed with a closed loop for the particle flow and an open end for the transport air. This arrangement ensures particle recycling via a cyclone back to the feeder without significant particle mass loss, for re-introduction at a controlled rate/concentration. For safety reasons the test plant was operated with glass beads of two different diameters instead of pulverized coal. Particle load and transport air velocity were varied during the test series in a range simulating that which naturally occurs with pneumatically transported coal (see test matrix, Figure 3.1 and Table 3.1).

### 2.1 The Testing Plant

The test duct layout is drawn in Figure 2.1. Two rotary piston blowers, operating in parallel and controlled by fan speed frequency converters, providing a velocity range of about 46 to 92 ft<sup>3</sup>/s for the transport air.

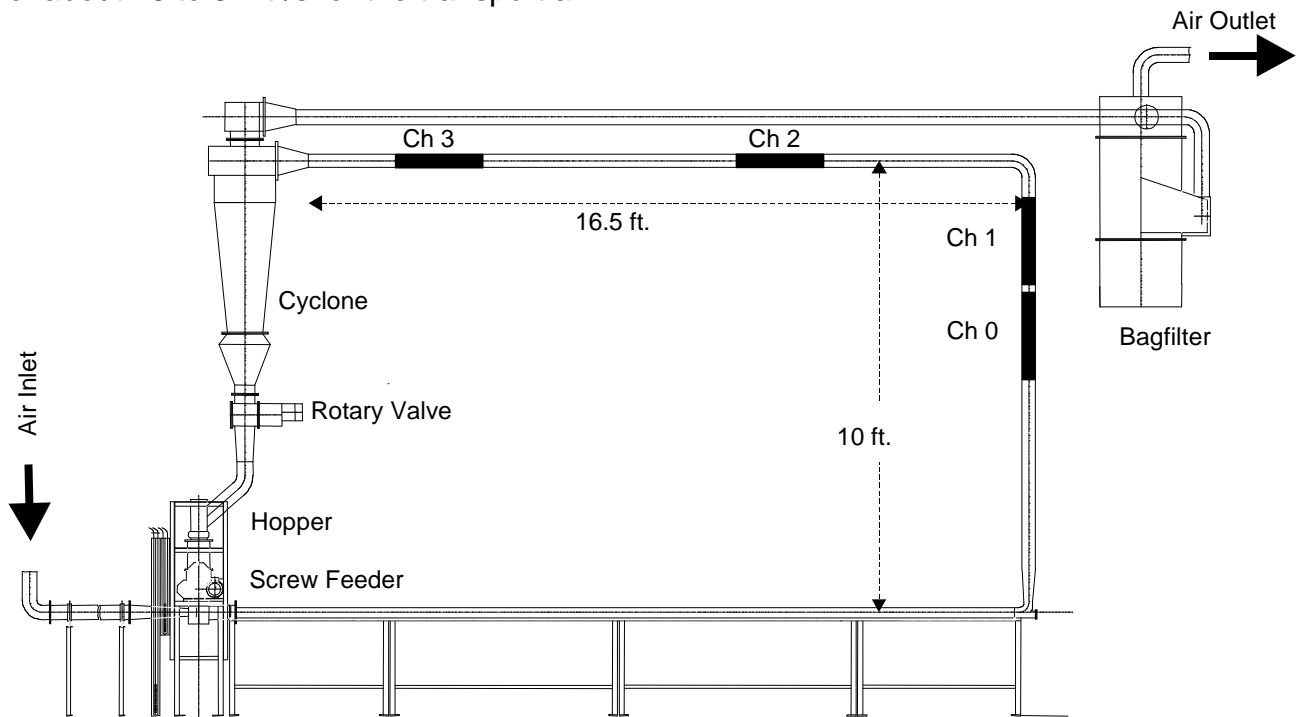


Fig. 2.1: Schematic drawing of the test plant

The particles are introduced to the airflow by a screw feeder, transported through the pipe and separated in a cyclone. Out of the cyclone the separated particles are fed

by a rotary valve back into the hopper of the screw feeder. The transport air is exhausted through a bag filter.

The screw feeder is frequency controlled over a range of 0 – 350 rpm. The horizontal run downstream of the feeder has a rectangular cross section, whereas the vertical and the upper horizontal pipes where the Pf-FLO measurements are located are round pipes having an inner diameter of 4.86”.

The airflow velocity is measured by a multi-point Pitot probe positioned upstream of the feeder. In addition, the airflow static pressure and temperature are also monitored.

## 2.2 The Pf-FLO Mass Flow Measurement

The Pf-FLO system independently measures the density and velocity of pulverized fuel in a two-phase flow. After a “zero” calibration of the empty transport pipe is performed for the density measurement process, absolute mass flow can be calculated using the product of the separate density and coal velocity signals.

### 2.2.1 Density measurement

Using the pipe as a wave-guide, the particulate concentration or density is measured with transmitted microwaves that cover the full cross section of the pipe. Starting with the known microwave transmission characteristic determined during empty pipe zeroing, the varying dielectric load caused by changing pulverized fuel (pf) concentrations produces a measurable frequency shift. The basics of this measurement can be described as follows<sup>1)</sup>:

The cut-off frequency ( $\lambda_{cut}$ ) of a round wave-guide is in this application the frequency of the H<sub>11</sub> mode. The wavelength of the H<sub>11</sub> mode is a function of the diameter of the pipe.

Equation 1. 
$$I_{cut} = \frac{p \cdot D}{X'_{mn}} = 1.71 \cdot D$$

wherein  $D$  is the diameter of the pipe and  $X'_{mn}$  is the solution of the Bessel function.

---

<sup>1)</sup> Kummer: Grundlagen der Mikrowellentechnik, chapter 3.4 and 4.3; Berlin: 1986

The frequency ( $f$ ) of the  $H_{11}$  mode depends on the dielectric  $\epsilon_r$  and the magnetic  $\mu_r$  properties of the volume in the wave-guide.

Equation 2. 
$$f = \frac{c}{\sqrt{\epsilon_r \mu_r} \cdot l_{cut}}$$
 where  $c$  is the constant for the speed of light

An unloaded pipe filled with air has a  $\epsilon_r$  of 1 and a  $\mu_r$  of 1. Hard coal has an  $\epsilon_r$  of 4 and  $\mu_r$  of 1. The volumetric ratio of pulverized coal to air at a coal concentration of 0.0312 lb/ft<sup>3</sup> is 1 to 2500. Since the resulting  $\epsilon_r$  changes between loaded and empty pipe in terms of 1/2500 the series expansion of Equation 2 can be used with its linear term. This gives a linear relation between the frequency and pf load within the concentration range typically found in coal fired power plants.

The Pf-FLO system couples microwaves in the range of the cut-off frequency into a pipe section using a pair of sensors, one sensor functioning as the transmitter and a second sensor as the receiver. The exact frequency of the  $H_{11}$  mode is calculated by scanning the transmitted microwave signal amplitudes.

A change in the concentration of pf in a given pipe changes the measured microwave frequency: The higher the concentration, the lower the frequency. The frequency shift caused by the pf is calculated by subtracting the frequency  $f_e$  of the loaded pipe from the frequency  $f_0$  of the empty pipe. This frequency shift is transformed into a density signal ( $r$ ) by the frequency density factor  $k_{fd}$ .

Equation 3. 
$$r = (f_0 - f_e) \cdot k_{fd}$$

Where  $f_0$  is determined by the empty pipe zeroing process.

Changes in pipe diameter caused by temperature do affect the measured frequency. Temperature compensation of the measured frequency uses the pipe surface temperature and the linear expansion factor for that pipe material.

## 2.2.2 Velocity measurement

The velocity measurement uses a cross-correlation method for comparing the stochastic signals of the electrostatic charged particles at two sensor locations of known separation (see Figure 2.2). An evaluation of the velocity sensor signals gives the time shift or time of flight ( $\tau_m$ ). Using the distance between the sensors ( $L$ ), solid particle velocity ( $v_s$ ) can be calculated as follows:

Equation 4. 
$$v_s = \frac{L}{t_m}$$

By using this method only particle velocity is measured, which in most instances differs from and is slower than the transport air velocity in a two-phase flow. This difference, or velocity slip, is a function of such factors as pipe configuration, specific weight and size of particles.

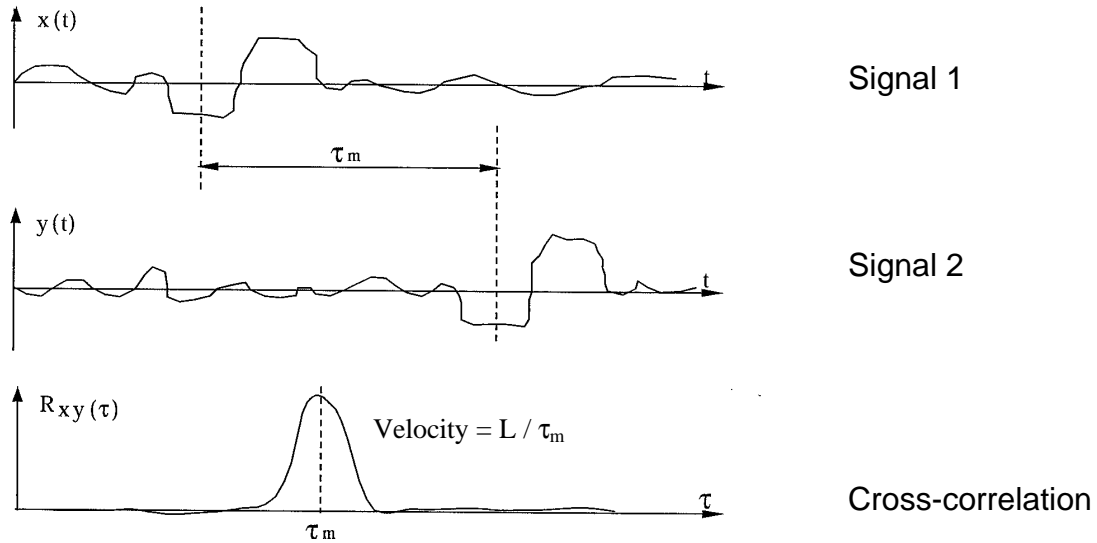


Fig. 2.2: Velocity measurement principle: signals and resulting cross-correlation function

### 2.2.3 Calculation of the Mass Flow

The mass flow  $\left(\frac{dm}{dt}\right)$  is calculated from the density and the particulate velocity

measurement as follows:

Equation 5. 
$$\frac{dm}{dt} = \mathbf{r} \cdot \mathbf{v}_s$$

The Pf-FLO system is calibrated to a known mass flow of the mill or pipe by adjusting the frequency density factor  $k_{fd}$  in Equation 3, which in turn depends on the pipe diameter. The factor  $k_{fd}$  is kept constant for all pipes with the same diameter.

## 2.3 Pf-FLO Test Configuration

The 4.86" diameter test duct pipe has a cut-off frequency of approximately 1.4 GHz. The standard microwave generating unit of the Pf-FLO system has been selected to provide frequencies up to only a 1 GHz level required for the range of larger coal pipe

sizes found in power plants. For the test runs conducted it was necessary to replace the standard model generator with a similar model having an extended frequency range of up to 2.0 GHz.

Corresponding to the smaller inner diameter of the test duct, the sensor antenna was also scaled down in length. Distances between sensors and rods in the test runs were the standard distances based on a pipe having a diameter  $D$ , as show in Figure 2.3.

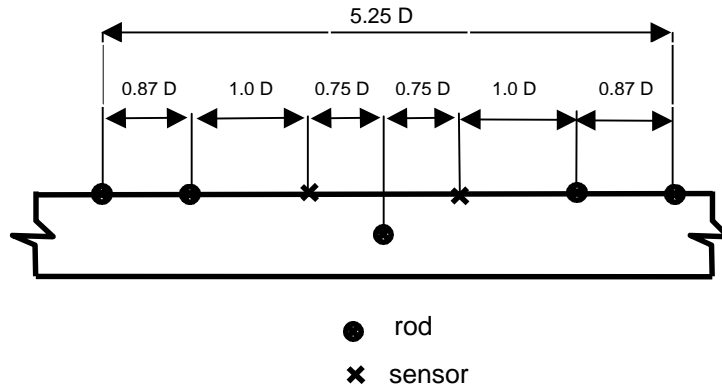


Fig. 2.3: Arrangement of sensors and rods at individual measurement locations

The Pf-FLO system uses wear resistant Tungsten Carbide rods to keep the propagation of the microwaves within the certain measurement zone of the pipe. Without the rods, the density measurement would be disturbed by reflected signals caused by pipe bends, orifice plates, isolation valves, etc., located upstream and/or downstream of the measurement zone. The optional fifth rod perpendicular to the sensors and located at their midpoint provides an additional signal short cut for depressing the propagation of  $90^\circ$  polarized  $H_{11}$  modes.

Without knowing the actual mass frequency factor for the test pipe size, all channels were initially set to

$$k_{fd} = 500 \left[ \frac{\text{a.u.}}{\text{Hz} \cdot \text{m}} \right]$$

This factor was kept constant for all measurements in the test. The resulting units for measured density ( $\rho$ ) and mass flow  $\left( \frac{dm}{dt} \right)$  are in arbitrary units [a.u.].

## 2.4 The Test Medium

The test plant could not be used with black coal for safety reasons. Therefore, glass spheres were used, with such properties as particle size, dielectric constant, and electrostatic charging similar to pulverized coal.

Typically 85 % – 95 % by weight of pulverized coal particles downstream of the mill's classifier are smaller than 90  $\mu\text{m}$  and 0.3 % or less are bigger than 225  $\mu\text{m}$ . The two glass particle sizes of 66  $\mu\text{m}$  and 225  $\mu\text{m}$  used for this test represent the main fraction and the biggest possible size fraction of particles in coal pipes.

The manufacturer of the glass beads specifies a glass density of 158.6  $\text{lb}/\text{ft}^3$  and an  $\epsilon_r$  of 2.28 at visible light. The  $\epsilon_r$  may be slightly different for microwaves due to dispersion.

The dielectric properties of milled coal and the glass spheres were tested in a microwave resonator chamber. It was found that the frequency shift in this measurement was dependent upon the dielectric properties on the bulk density of the pulverized medium. By calculating the frequency shift per mass, the influence of the sphere packing were eliminated. The results are displayed in Table 2.1.

Medium	Bulk density [ $\text{lbs}/\text{ft}^3$ ]	Frequency shift/ mass [MHz/lb]
Glass spheres	88.1	124.1
Black coal (Primero)	35.8	200.1
Black coal (Blumenthal)	35.8	193.9
Black coal (Knurrow)	41.8	193.5

Table 2.1: Bulk density and frequency shift for fixed-bed powder of pulverized black coal and glass particles

The frequency shift at the same mass flow caused by glass is about 2/3 of the tested coal. Therefore, the expected frequency shift for the mass flow measurement will only be about 1/3 less for glass than for coal with the same mass. This ensures a good comparability between the test data obtained with glass particles used as the test medium versus that which would have been obtained had coal been able to be used for the test medium.

The density for raw coal is between 78.0 and 81.8  $\text{lbs}/\text{ft}^3$ . Taking this density into account, glass particles of the same size are about two times heavier than coal

particles. The weight differential plus the shape of the particles, spherical for glass and polyhedral for coal, give glass aerodynamic properties which result in a greater velocity differential or slip between the airflow and the glass particles.

The electrostatic charging depends on particle collisions and particle conductivity. The velocity measurement needs a certain amount of electrostatic charge to correlate the sensor signals into a reliable time of flight measurement. Charging signal strengths for both size glass beads and bead mixtures were sufficiently high to obtain accurate time of flight measurements. Induced by the substantially greater number of particle amount within the airflow, the signal strength of 66  $\mu\text{m}$  particles was about five times higher than for the 225  $\mu\text{m}$  particles.

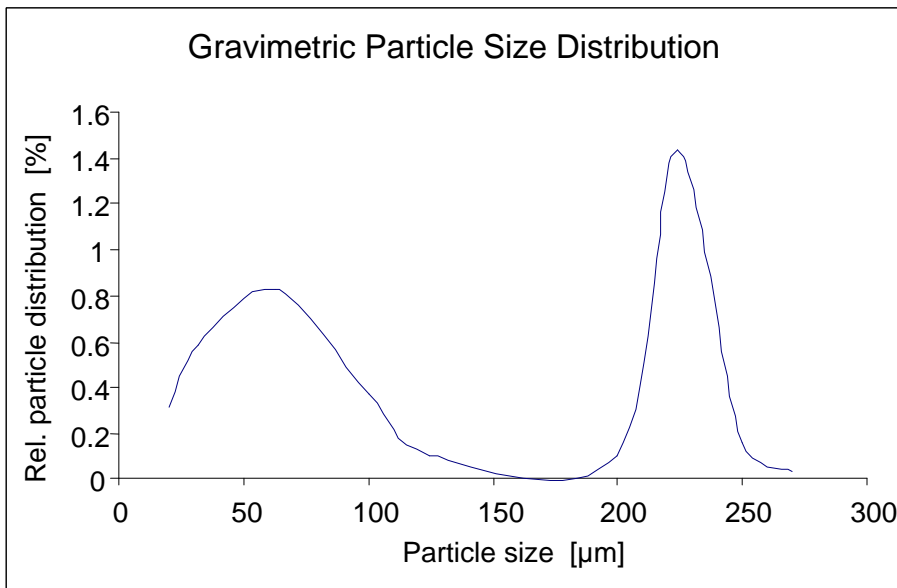


Fig. 2.4: Particle distribution as a function of particle size for the 50/50 mix of 66  $\mu\text{m}$  and 225  $\mu\text{m}$  particles

Beside the pure 66  $\mu\text{m}$  and 225  $\mu\text{m}$  particles, a 50/50 mix by weight was also tested. Figure 2.4 shows the gravimetric distribution of particle sizes.

## 2.5 Feeder Calibration

To calibrate the feeder, glass beads were fed by the frequency controlled feeder into a container for 30 seconds and their mass was weighed. This procedure was repeated twice for each particle size in steps of 50 rpm from 0 to 350 rpm. The average of both sets of measurements was used for the feeder calibration.

The repeatability of the feeder calibration was then tested by 10 individual measurements with the 66  $\mu\text{m}$  particles at 150 rpm. They were all in the range of  $\pm 0.9\%$  by weight.

This was acceptable since the aim of the tests was not to examine the characteristics of the screw feeder. And with all four sensor locations measuring physically the same airflow/particle mixture, any scattering of the feeder is eliminated as a common variable.

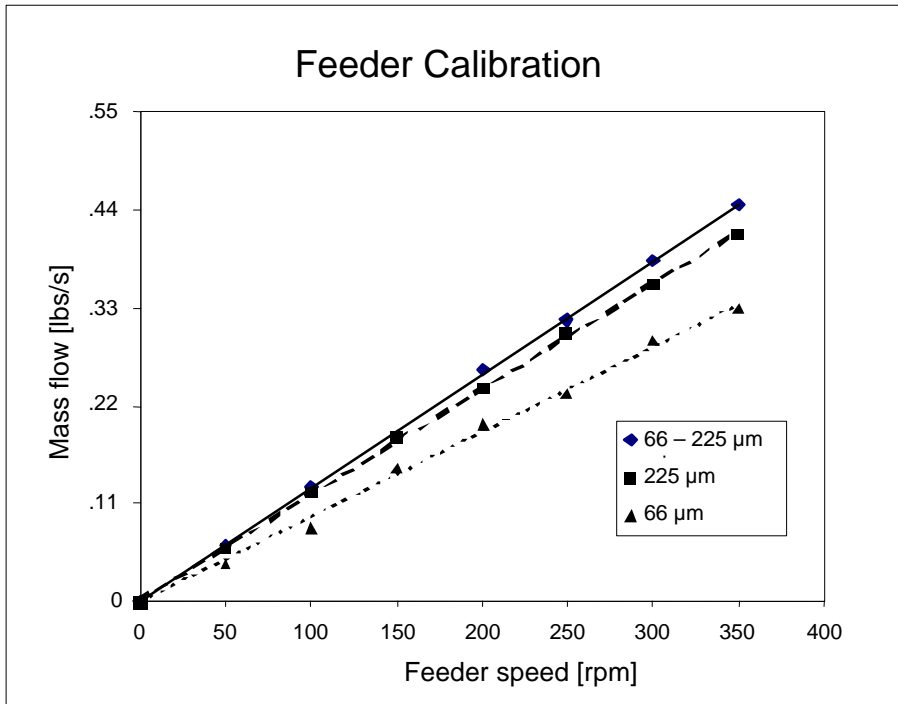


Fig. 2.5: Mass flow versus feeder speed for different particle fractions

The mass flow of the feeder is shown in Figure 2.5 for the specific particle fractions. The mass flow at a particular feeder speed depends on the particle size distribution. The mix of the two size fractions has the tightest packing and thus shows the highest mass flow. The 66  $\mu\text{m}$  and 225  $\mu\text{m}$  particles have different mass flows since for particles  $< 100\ \mu\text{m}$ , adhesion forces influence the flowability within the screw feeder.

### 3. Testing Procedure

The test runs have been made under the aspect of realistic airflow velocities and particle concentrations.

Within the capacity of the fan, three velocity levels were chosen at 72 ft/s, 82 ft/s, and 92 ft/s, representing normal transport velocities in utility plants. With constant air velocities the feeder speed was varied between 0 - 300 rpm in steps of 50 rpm.

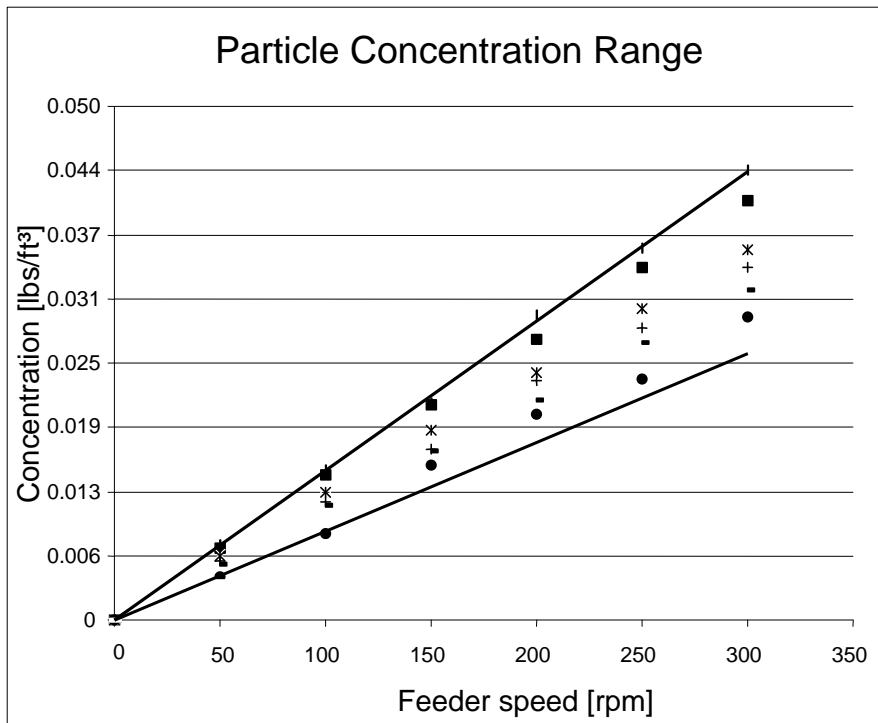


Fig. 3.1: Range of pf-concentrations based on feeder mass flow and transport air flow

The pf concentrations in utility plants usually range between 0.012 to 0.031 lbs/ft<sup>3</sup>. Figure 3.1 shows the range of the expected pf concentration based on the ratio of feeder mass flow and the airflow during the tests.

Table 3.1 gives an overview of the different test runs: From the total number of 15 test runs there were six runs with the 66 μm particles, six runs with the particle mix and three runs with the 225 μm particles.

Particle Size	Test Numbers		
66 $\mu\text{m}$	I,VI	II,V	III,IV
225 $\mu\text{m}$	I	II	III
66 - 225 $\mu\text{m}$ mix	I,IV	II,V	III, VI
	72 ft/s	82 ft/s	92 ft/s
	Gas Velocity		

Table 3.1: Test run number for each particle size

The following diagrams illustrate the data acquired for all test runs: Diagram Figures 3.2 and 3.3 show density and velocity measurement, and Figure 3.4 shows the resulting mass flow of the 66 – 225  $\mu\text{m}$  particles of Test Number V. Each feeder step was kept constant for at least 15 minutes to get about 20 individual measurements. From the last 15 measurements of each feeder step the average was taken and plotted against the feeder mass flow in Figure 3.5.

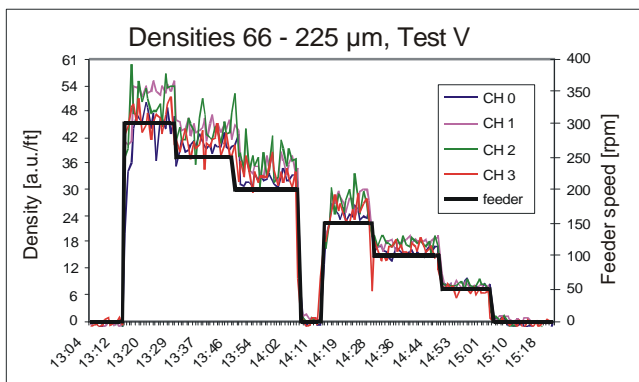


Fig. 3.2: Density measurement

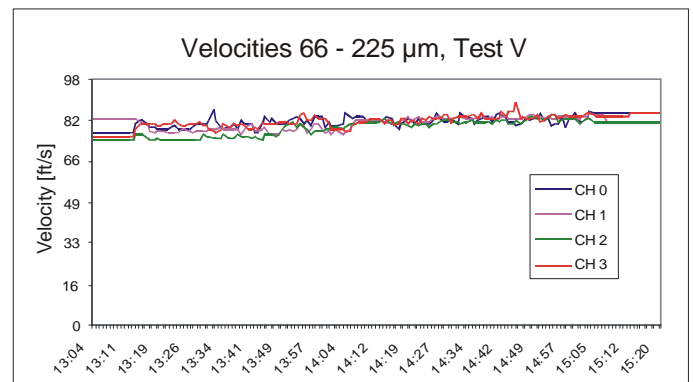


Fig. 3.3: Velocity measurement

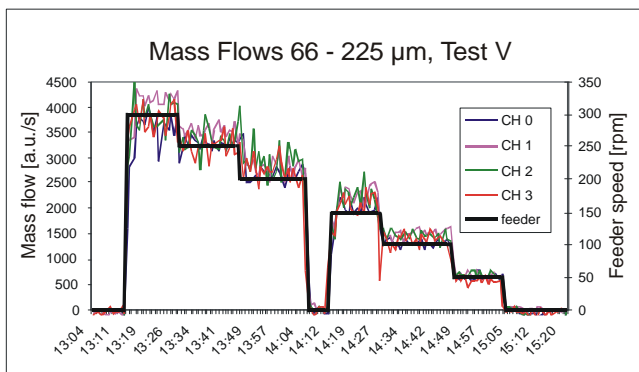


Fig. 3.4: Resulting mass flow and feeder signal

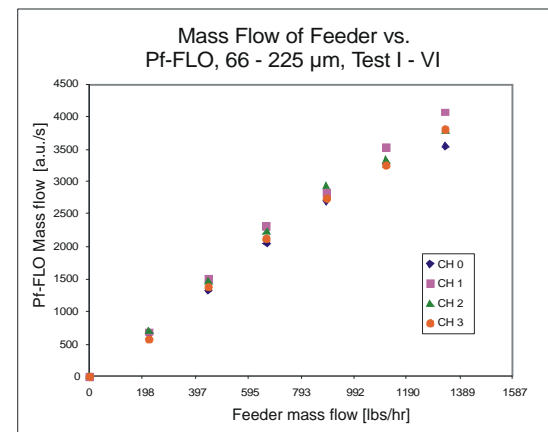


Fig. 3.5: Mass flow of feeder versus Pf-FLO

All test runs have been plotted as displayed in Figure 3.5. As there is only a constant factor between [a.u./s] and [g/s], a unified y-axis scaling was used to help evaluate the influence of different particle sizes (see also Figure 4.8).

## 4. Results

### 4.1 Pf-FLO Measurement Accuracy

Figures 4.1 and 4.2 illustrate results only for the 50/50 particle mix. Results for other particle fractions are listed in the tabulations in Sections 4.1.1 and 4.1.2.

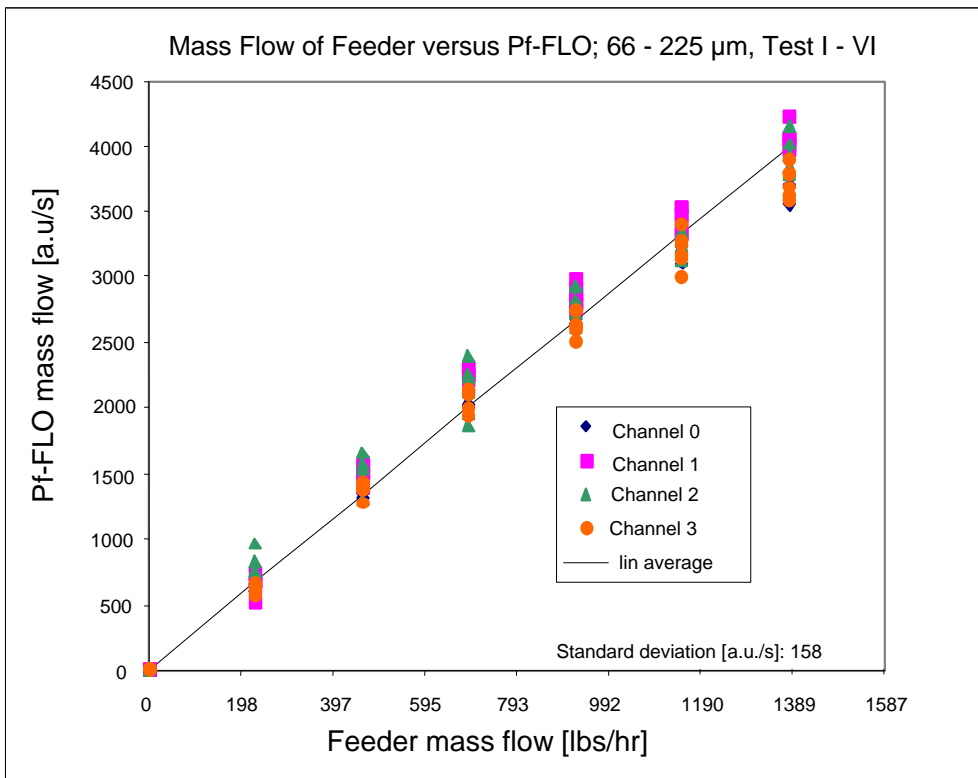


Fig. 4.1: Evaluation of all test runs with 66 / 225  $\mu\text{m}$  particles

The diagram in Figure 4.1 shows the evaluated results for all measuring channels versus the feeder mass flow. The mass flow signals of all channels were averaged for each feeder step and one particle fraction, and a linear coefficient was determined for it. With this coefficient the linear average was calculated as it can be seen in the diagram, indicated with “lin. average”. Based on the linear average the standard deviation was determined for each measuring channel as listed in Table 4.1.

The repeatability of one channel for all tests and one particle size is exemplarily displayed in Figure 4.2. For other measuring channels and particle fractions, see tabulations in Section 4.1.2.

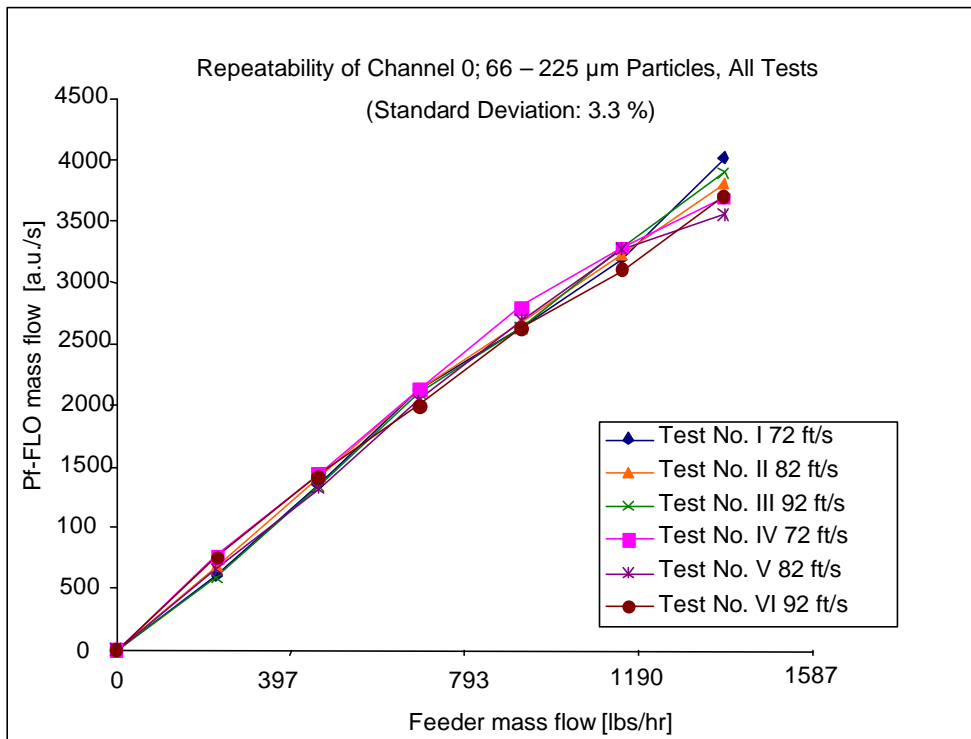


Fig. 4.2: Repeatability of channel 0 for 66 - 225  $\mu\text{m}$  particles

### 4.1.1 Absolute Deviation

The standard deviation of one particle fraction from the linear average of all channels is listed in Table 4.1. The errors in % refer to the maximum mass flow determined at 300 rpm feeder speed.

Particle Size	Channel	Test No.	Number of Measurements	Standard Deviation [a.u./s]	Max. Mass Flow [a.u./s]	Mean Error %
66 $\mu\text{m}$	CH0 - CH3	Test I - VI	144	109	2462	4.4%
225 $\mu\text{m}$	CH0 - CH3	Test I - III	72	132	3520	3.8%
66 - 225 $\mu\text{m}$	CH0 - CH3	Test I - VI	144	158	4000	3.9%

Table 4.1: Standard deviation and mean error for individual particle fractions

## 4.1.2 Repeatability

The relative deviation of one channel in all tests shows its repeatability. This includes the scattering of the feeder but excludes systematic deviations from one channel in comparison to the others. Results for each channel are listed in the Tables 4.2 to 4.4.

Channel	Test No.	Number of Measurements	Standard Deviation	
			To Linear Average [a.u./s]	Mean Error %
CH 0	Test I - VI	36	75.1	3.1%
CH 1	Test I - VI	36	92.5	3.8%
CH 2	Test I - VI	36	93.4	3.8%
CH 3	Test I - VI	36	72.9	3.0%

The error in % refers to the maximum mass flow at 300 rpm: 2462 [a.u./s]

Table 4.2: Standard deviation of the individual channels with 66  $\mu\text{m}$  particles

Channel	Test No.	Number of Measurements	Standard Deviation	
			To Linear Average [a.u./s]	Mean Error %
CH 0	Test I - III	18	132.3	3.8%
CH 1	Test I - III	18	65.0	1.8%
CH 2	Test I - III	18	151.9	4.3%
CH 3	Test I - III	18	111.7	3.2%

The error in % refers to the maximum mass flow at 300 rpm: 3520 [a.u./s]

Table 4.3: Standard deviation of the individual channels with 225  $\mu\text{m}$  particles

Channel	Test No.	Number of Measurements	Standard Deviation	
			To Linear Average [a.u./s]	Mean Error %
CH 0	Test I - VI	36	131.7	3.3%
CH 1	Test I - VI	36	114.1	2.9%
CH 2	Test I - VI	36	163.9	4.1%
CH 3	Test I - VI	36	141.2	3.5%

The error in % refers to the maximum mass flow at 300 rpm: 4000 [a.u./s]

Table 4.4: Standard deviation of the individual channels with 66-225  $\mu\text{m}$  particle mix

## 4.2 Influence of the Particle Size

Another purpose of the tests was to quantify the influence of particle sizes. As the 225  $\mu\text{m}$  particles can only be found in smaller percentages in pulverized coal, it is a practical fraction to resolve particle size dependent influences on density and velocity measurement. The transferability of the results to the operating condition of coal fired power plants have to be viewed in relation to the real particle size distributions in coal pipes. In Section 4.2.3 the results out of the tests are evaluated.

### 4.2.1 Velocity Measurement

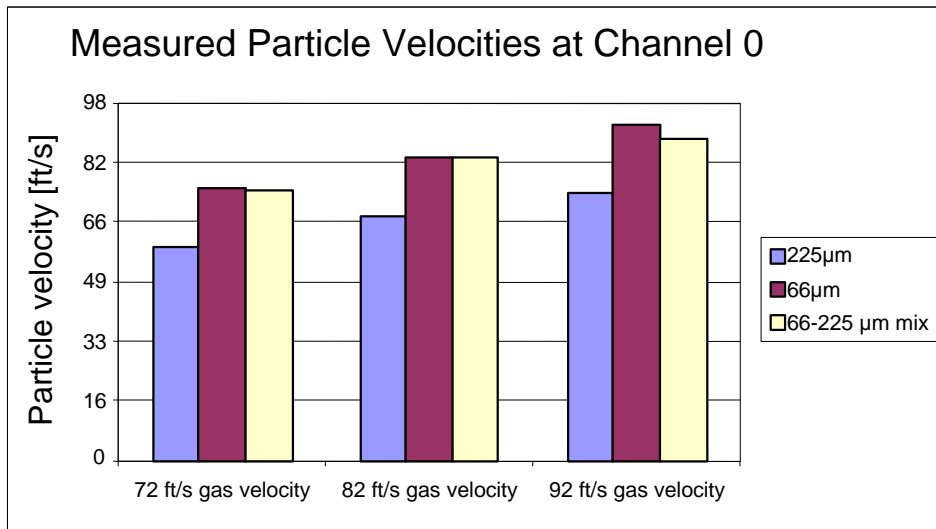


Fig. 4.3 Averaged particle velocities at channel 0

The measurements with 225  $\mu\text{m}$  particles showed a difference of about 16.4 ft/s between airflow and particle velocity. This is due to the change in the aerodynamic properties which increase the slip between particles and gas. The weight of particles changes proportional to  $D^3$  but the cross section only changes proportional to  $D^2$ .

The velocity of the 66  $\mu\text{m}$  particles, as well as the 50/50 mix, was found to be very close to the airflow velocity. The reason can be found by comparing the electrostatic signal strength. The electrostatic signal strength of the 225  $\mu\text{m}$  particles was found to be significantly lower than for 66  $\mu\text{m}$ . But the particle number increases with the relation of particle diameters to the power of three (see above). With a 50/50 particle mixture by weight, the number of 66  $\mu\text{m}$  particles is about 28 times greater than for the 225  $\mu\text{m}$  particles. The cross correlation method resolves the time shift of the sensor signals by comparing their highest identity. If the signal strength of two time

shifts is of the same order, it might be possible to distinguish between the two velocities. In case of the particle mix the signal strength of the 225  $\mu\text{m}$  particles was below the noise signal level of the 66  $\mu\text{m}$  particles. Therefore, it is obvious that only the velocity of the 66  $\mu\text{m}$  particles has been measured. The error in relation to the realistic particle size distribution is estimated in Section 4.2.3.

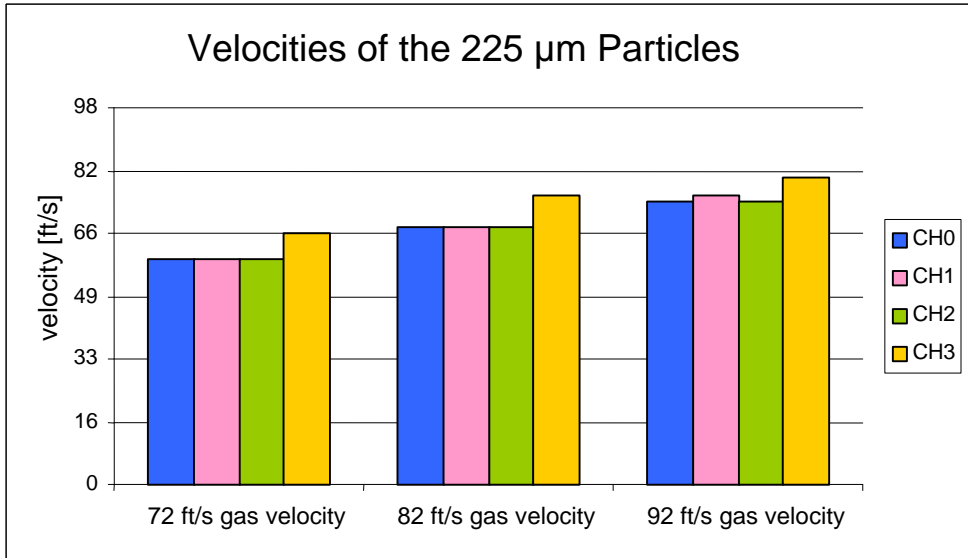


Fig. 4.4: Acceleration along the test duct of the 225  $\mu\text{m}$  particles

In the tests which measured 225  $\mu\text{m}$  particles only, channel 3 was found to have higher velocities than the other channels. This can be explained by the position of this sensor pair located at the end of the horizontal test duct with the longest straight run after a bend (see Figure 2.1). This leads to a certain acceleration, especially for the bigger sized particles.

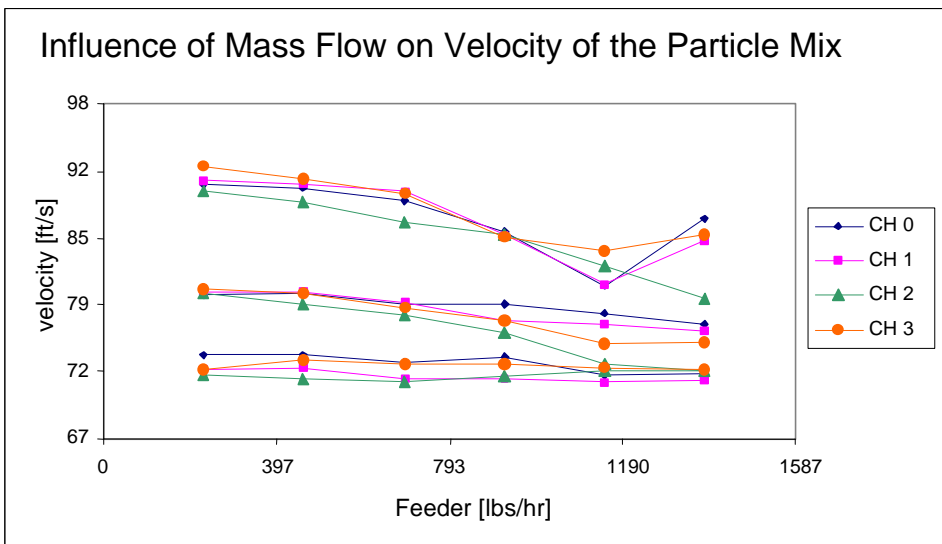


Fig. 4.5: Influence of the mass flow on the velocity of the particle mix in Test IV-VI

Figure 4.5 shows the influence of the mass flow on particle velocity. This effect, here illustrated for the particle mix, is obvious when the averaged velocity of each feeder step is plotted over the mass flow as it is done in Figure 4.5. Each bundle of the four channels represents one step of the airflow velocity.

The higher the airflow velocity the higher the influence from pf load in the pipe. Channel 2 with the shortest distance from a bend seems to be affected most. It is assumed that this effect is related to particle interaction between 66  $\mu\text{m}$  and 225  $\mu\text{m}$  particles, the latter having significantly lower velocities.

### 4.2.2 Density Measurement

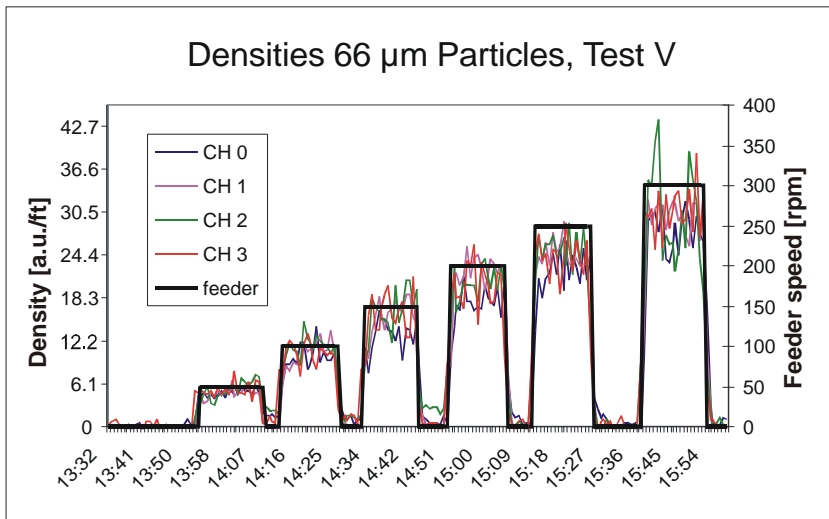


Fig. 4.6: Density measurement with 66  $\mu\text{m}$  particles Test V.

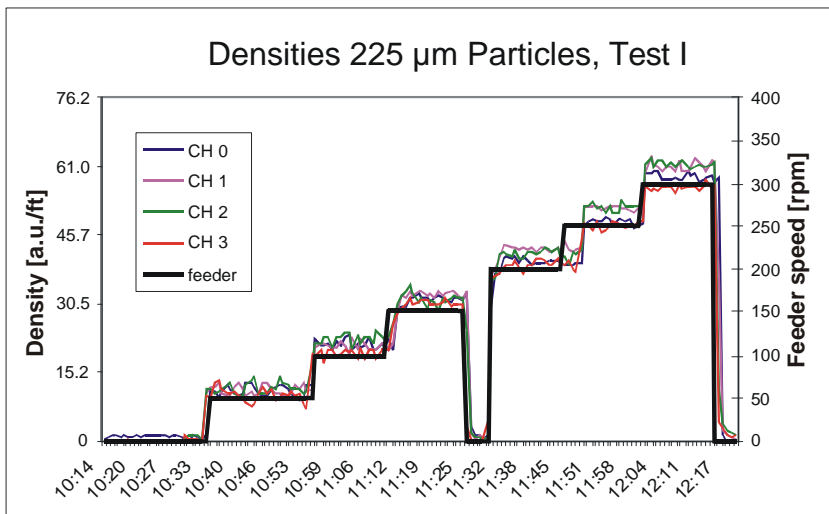


Fig. 4.7: Density measurement with 225  $\mu\text{m}$  particles Test I

The diagrams in Figures 4.6 and 4.7 show the particle size dependent scattering of the densities in two test runs. The more extended scattering of the density signal for 66  $\mu\text{m}$  particles also increases with the load or particle numbers. With the 225  $\mu\text{m}$  particles there was less scattering although the densities in Figure 4.7 were nearly twice as high. The fluctuation quantity for the particle mix is higher than the one for the 225  $\mu\text{m}$ , but less than the one for the 66  $\mu\text{m}$  particles and was also influenced by the load (see Figure 3.4).

The scattering of measurement is proved to be realistic and relates to the density fluctuations of the particle flow. The different behavior can be explained with the mean free path between particle collisions. The 66  $\mu\text{m}$  particles have less particle-wall collisions but more particle-particle collisions in a smaller volume. Local high and low density concentrations do not average out within the pipe volume that has been measured.

### 4.2.3 Mass flow measurement

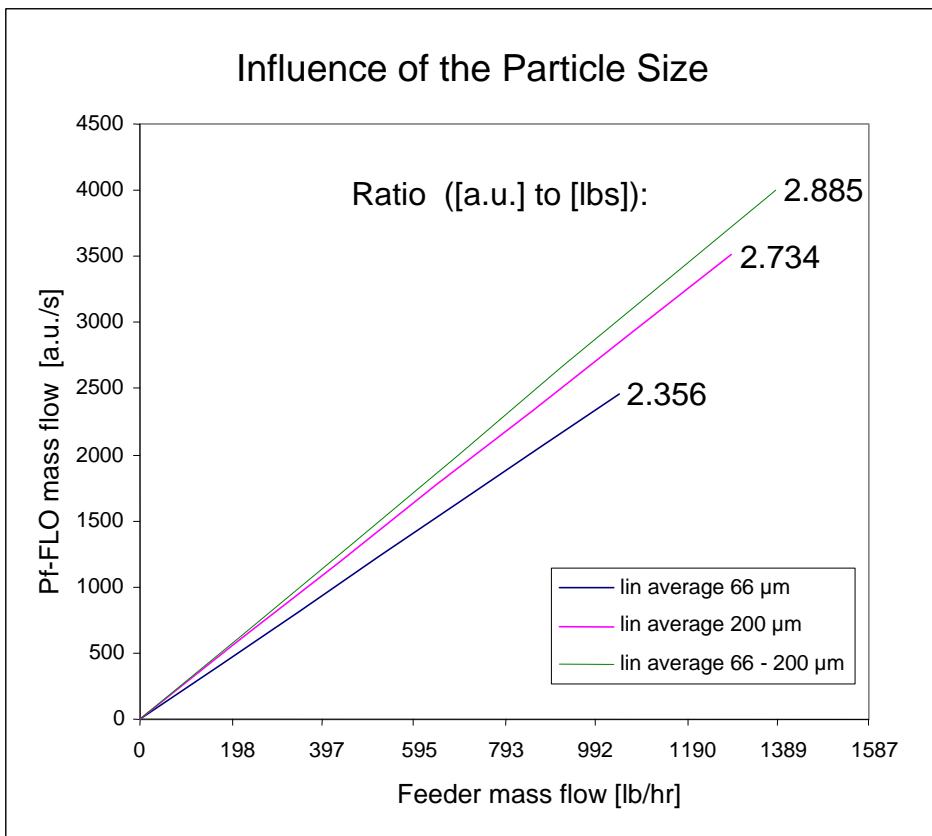


Fig. 4.8: Influence of the particle size on the Pf-FLO measurement

The diagram in Fig. 4.8 shows the ratio of arbitrary units [a.u./sec] to mass [g] taken from the linear averages of the four measurement channels. This factor was found to be a function of the used particle fraction. The temporarily applied ‘arbitrary units’ to ‘frequency factor’ of 500 (see section 2.3) has to be divided by this ratio to get the calibrated mass flow signal for each particle fraction. The resulting  $k_{fd}$  is displayed in Table 4.5.

Particle Fraction	ratio [a.u./lbs]	$k_{fd}$ [g/m kHz]
66 $\mu\text{m}$ particles	2.3562	26.7
225 $\mu\text{m}$ particles	2.7342	23.0
66-225 $\mu\text{m}$ particle mix	2.8854	21.8

Table 4.5: Ratio of arbitrary units to mass and the resulting mass frequency factor  $k_{fd}$  for each particle fraction

The deviation of 13.8 % between the 66 and 225  $\mu\text{m}$  particles can be regarded as dependent on particle size. The deviation of the 66 – 225  $\mu\text{m}$  particle mix is due to the deviation of the velocity measurement described in Section 4.2.1.

The results have to be compared with the real particle size distribution in a coal pipe after classifier. These deviations have influence only on the absolute accuracy but not on the relative accuracy between several pipes of one mill since a segregation of particle fractions between several pipes is not probable.

The following calculations are linear estimations of the error in real particle size distributions within the results of the tests: For an exemplary particle distribution of 15% >90  $\mu\text{m}$  and 0.2 % >225  $\mu\text{m}$  it was assumed to have a discrete mixture out of 84.8 % 66  $\mu\text{m}$  particles, 15 % 145  $\mu\text{m}$  particles and 0.2 % 225  $\mu\text{m}$  particles. The relation of the diameters was taken to interpolate the velocity of the 145  $\mu\text{m}$  particles linear between the velocities of the 66  $\mu\text{m}$  and 225  $\mu\text{m}$  particles. Also the relation of the diameters was taken to interpolate the deviation of density measurement for 145  $\mu\text{m}$  particles linear between the densities of the 66 and 225  $\mu\text{m}$  particles.

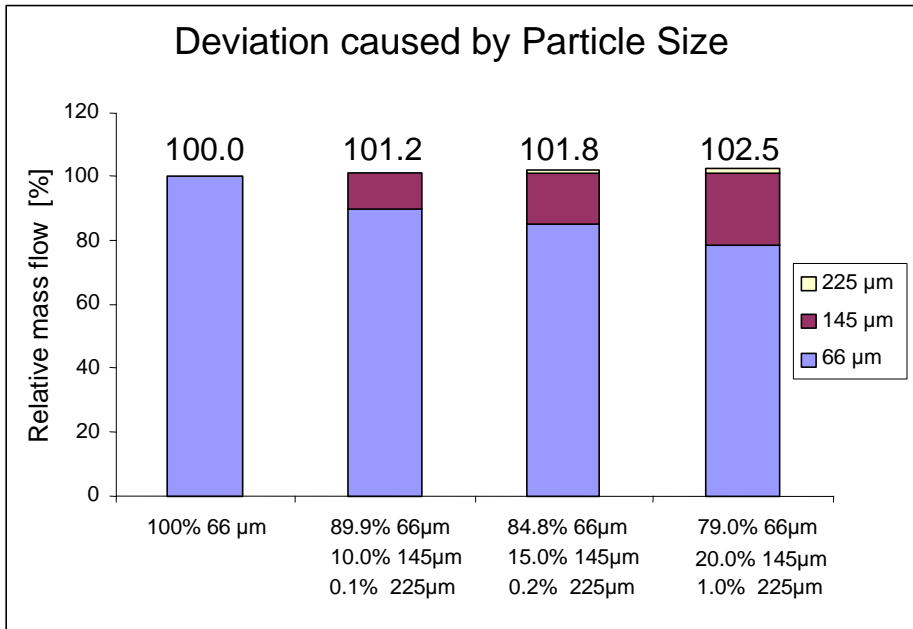


Fig. 4.9: Estimated deviation by modeled particle size distribution

The results of the estimation are shown in Figure 4.9. If the distribution changes from column 2 to 3, the estimated error is about 0.6 % of the mass flow. The distribution of the last column shows a 2.5 % error but this change in particle distribution is meant to be quite unrealistic in an optimized milling process and will also influence the combustion badly.

## 5. Abstract

A reference test at the pneumatic conveying test plant of the “Lehrstuhl für Mechanische Verfahrenstechnik” at the University of Halle-Wittenberg was established to prove the accuracy of a flow measurement system for air-solid flows. The test facility consists of a calibrated screw feeder, a pipe system with vertical and horizontal elements, and the particle separation equipment. Glass beads were used as a test medium whose physical properties are comparable to coal dust if taking into account the measurement principle. In addition to the single sized test materials with diameters of 66  $\mu\text{m}$  and 225  $\mu\text{m}$ , a 50/50 mixture by weight of both particle sizes was used. The experimental matrix for the tests covered the usual operational range for the throughput and the velocity in coal pipes of power plants.

In total, four measurement instruments were located at two locations in the upward run and two locations in the horizontal run of the test pipe. From the measured density and velocity signals of the particles the mass flow was calculated in each case and compared with the calibrated feeder signal. The measuring error was related to a single standard deviation.

As a result, the measured deviation from the feeder signal is  $< 4.5 \%$ ; this applies to the entirety of all four measuring points and all particle fractions. For individual sensors the deviation lies in the range between 1.8 % to 4.3 %, and is in this case not significantly dependent on the used particle size.

In addition, investigations of the influence of the particle size were carried out. Within the wide range of the used particle fractions, the density and velocity measurement showed some size dependencies. However, the measured differences have only little influence on the accuracy ( $< 0.6 \%$ ) since in utility plants the grading of coal dust usually changes only in a comparable small range.